Characterization of ^{10}B targets at ILL

E. Berthoumieux, G. Tsiledakis, E. Dupont, F. Gunsing
CEA Irfu, University Paris-Saclay, F-91191 Gif-sur-Yvette, France

D. Vendelbo, P. Schillebeeckx, R. Wynants
European Commission, Joint Research Centre (JRC), B-2440 Geel, Belgium

J. Marchal, B. Guérard
Institut Laue-Langevin (ILL), 71 Avenue des Martyrs, F-38000 Grenoble, France

July 19, 2024

Abstract

The areal density of several ^{10}B samples, produced at JRC-Geel, has been determined relative to a reference sample at the Institut Laue–Langevin (ILL) in Grenoble, using an automated scanning device from JRC-Geel with a $LaBr_3$ detector. For each sample, several points were irradiated by 13.1 meV neutrons and the resulting gamma-ray spectra were recorded. The intensity of the 478 keV gamma rays from the ^{10}B(n,$\alpha\gamma$)^{7}Li reaction was determined.

Introduction

The present experiment consists of measuring the gamma-ray spectra of several ^{10}B samples, all manufactured at JRC-Geel, with a narrow-diameter neutron beam and a device to move each sample in directions perpendicular to the neutron beam. The aim is twofold: first, to determine the average areal density relative to a reference sample, and second, to quantify the homogeneity of each sample over the sample surface. The ^{10}B samples are used in different types of neutron detectors sensitive to the produced α and ^{7}Li particles. These detectors either measure the neutron flux integrated over the ^{10}B sample area, or measure the neutron beam profile by means of an XY-readout based on perpendicular detection strips. The latter detector is currently under development in a common project between JRC-Geel and CEA Saclay. For this detector which has a positional readout with a resolution of about 1×1 mm^2, a measure of the homogeneity over the sample surface is of importance. We use the word sample in this report since in the context of an accelerator-based neutron source, the in-beam targets are usually called samples to distinguish them from the neutron-producing target.

gunsing@cea.fr

Table 1. The ^{10}B samples available for the present measurements with their nominal areal densities. The three numbers listed under "dimensions" correspond to the diameters of the boron deposit and of the support ring as explained in the text.

sample	nominal areal density ^{10}B (μg/cm^2)	dimensions (mm)
TP2021-008-05	$\sim$26	90, 100-120
TP2021-008-06	$\sim$30	90, 100-120
TP2021-008-07	$\sim$25	90, 100-120
TP2021-008-08	$\sim$5	90, 100-120
NS00041	81.8 ± 7	84, 108-128
FP15-030	$\sim$80	84, 108-128
TP2012-001-01	8.766 ± 0.138	37.97, 108-128

The experiment at ILL, approved under **TEST-3322**, uses a scanning device developed at JRC-Geel, into which the ^{10}B samples can be mounted facing a pencil neutron beam, and automatically be positioned according to a user-defined pattern with a stepping size down to 1 mm and a repeatable positioning accuracy of 1 μm. The 478 keV gamma ray from the ^{10}B(n,$\alpha_1\gamma$)^{7}Li reaction, which accounts for 95% of the total ^{10}B(n,α) reaction, is measured with a $LaBr_3$ detector, mounted in a fixed position facing interaction point of the beam and the sample. In this way, the gamma-ray spectrum for each position of the sample is recorded for off-line analysis.

1 Samples

A number of boron samples, highly enriched in ^{10}B, all produced at JRC-Geel, have been used in the present measurements. A set of recently manufactured samples, with sample IDs **TP2021-008-**nn, are 90 mm diameter pure boron deposits on aluminized mylar (9 μm), spanned on an aluminium ring with internal and external diameter of 100 and 120 mm respectively. The approximate areal densities are given in table 1.

The sample with ID **NS00041** has two 84 mm diameter back-to-back spots of boron (enrichment 94% ^{10}B) on a 30 μm thick aluminium foil, glued on a 0.5 mm stainless steel ring with internal and external diameter of 108 and 128 mm respectively. The B areal densities of the two sides are documented as 46 ± 5 and 41 ± 5 μg/cm^2 without further specifications. Therefore we consider the total areal density of ^{10}B as $0.94 \times 87 \pm 7 = 81.8 \pm 7$ μg/cm^2.

The sample with label **FP15-030** is composed in a similar way with the same dimensions and two deposits, each on one side. The areal density is approximate 80 μg/cm^2.

Finally the sample with label **TP2012-001-01** has the same stainless steel ring with internal and external diameter of 108 and 128 mm respectively, but now with a sample spot diameter of 37.97 mm. The areal density is 8.766 ± 0.13 μg/cm^2. The total mass of ^{10}B of the sample has been calibrated with in a previous (n,α) experiment. This sample is considered to have a reference areal density.

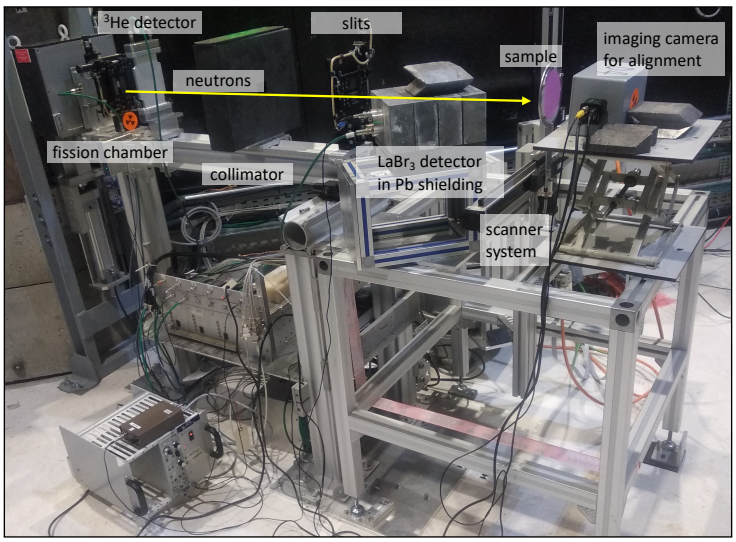

Figure 1. The experimental setup.

2 Experimental setup

The experiment was performed at beam line CT2 of ILL. The neutron fluence rate at this beam line is approximately 1.5×10^6 neutrons cm^{-2}s^{-1} for neutrons with a kinetic energy of 13.1 meV (wavelength 2.5 Å). At this energy the cross section of the ^{10}B(n,α) reaction is about 5343 b (calculated using ENDF/B-VIII.0 evaluated data), from which 95% corresponds to the ^{10}B(n,$\alpha_1\gamma$)^{7}Li reaction emitting a 478 keV gamma ray. The beam line has adjustable perpendicular B_4C slits in order to collimate the beam to a rectangular shape. A ^{235}U fission chamber was placed upstream in the beam and used as a counter to monitor the incident neutron flux. A ^{3}He detector was also placed upstream in the beam but not used. Only at the end of the experiment, the ^{3}He detector was placed behind the sample in order to measure neutron transmission information.

A scanning device developed and tested at JRC Geel was placed in the beam. The device consists of an adjustable aluminium frame containing a remotely controllable stepping motor device, driving a sample holder. A BrilLanCe-380 detector consisting of a 2×2 inch $LaBr_3$(Ce) crystal, coupled to a XP5500B photomultiplier tube and a AS20 voltage divider, was also fixed on the frame. The equipment was driven by the DAQ2000 data acquisition system which allowed for placing the sample in a certain position, taking the gamma-ray spectra measured by the $LaBr_3$ detector, and recording the connected neutron counting detectors. Sequences of stepping actions allowed to automatically perform a scan of the sample in a user-defined configuration. In figure 1 a picture of the setup is shown.

3 Measurements of ^{10}B(n,$\alpha_1\gamma$) gamma rays

Once a particular sample was mounted in the scanning device, the starting position, unfortunately not automatically recorded by the system so manually documented, the number of steps, the spacing between steps, and the run time were set. Then, for each position, a gamma-ray spectrum was recorded by the DAQ2000 system. For all sample, background, and test measurements, this resulted in more than 2100 acquired spectra.

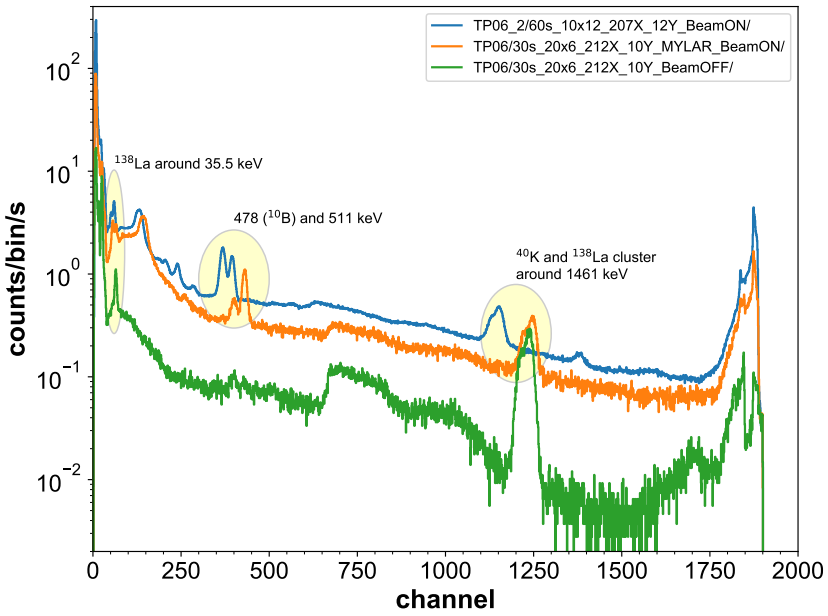

Figure 2. Examples of global gamma-ray spectra, summed for all positions, for beam-off, and beam-on with and without a ^{10}B sample. The intrinsic background of the $LaBr_3$ crystal allows for an accurate energy calibration. A change in the calibration can be clearly seen from the change in position of the characteristic peaks.

In figure 2 we show global gamma-ray spectra, summed over all positions and acquired for beam-off, and for beam-on with and without a ^{10}B sample. The typical background largely due to the intrinsic background from the $LaBr_3$ crystal, mainly ^{138}La, ^{227}Ac, and others, is clearly visible all spectra. For the beam-on spectra, additional, prominent peaks appear. The region of interest of the spectra was situated around the two gamma-rays corresponding to the 478 keV peak from ^{10}B(n,α) and the 511 keV annihilation peak. No other gamma rays were identified in the vicinity of those peaks.

Nevertheless, we observed a change in gain over time, both for the 478 keV and for the 511 keV peak, which complicated an automatic fitting procedure. Eventually we implemented a peak

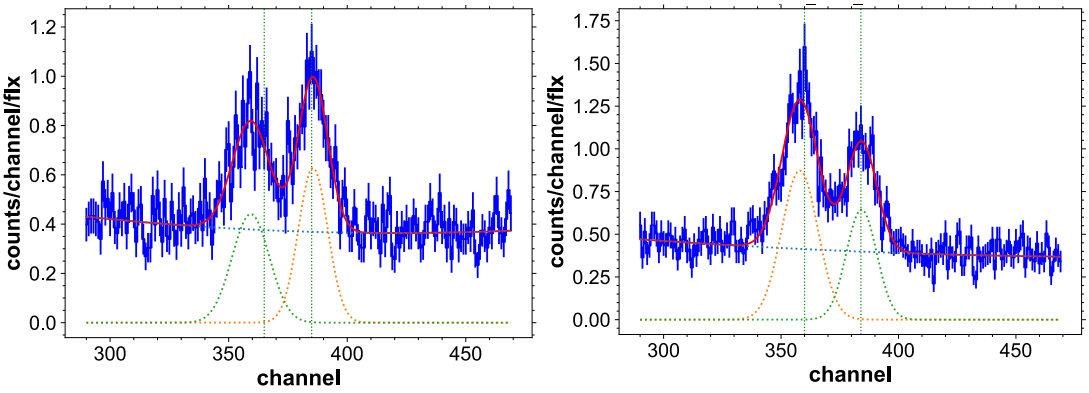

Figure 3. Typical gamma-ray spectra (blue) showing the 478 and 511 keV peaks together with a fit (red) and the components of the fit (dotted). The left panel is for a spectrum without a sample, while the right panel is for a spectrum with a ^{10}B sample in the beam.

search in the region of interest in order to obtain reasonable initial guesses for the subsequent non-linear fit. The fit model consisted of two Gaussians on top of a second order polynomial background. In the fit, all parameters were left free. We then calculated the peak area and its uncertainty using proper uncertainty propagation from the fitted parameters, including the correlation between the width and the height of the peak. The peak area was normalized in order to be proportional to the incident neutron flux measured by the upstream neutron counter. In figure 3 we show a typical gamma-ray spectrum showing the position of the initial guess of the peak positions, and the final fits and their components of the 478 and 511 keV peaks.

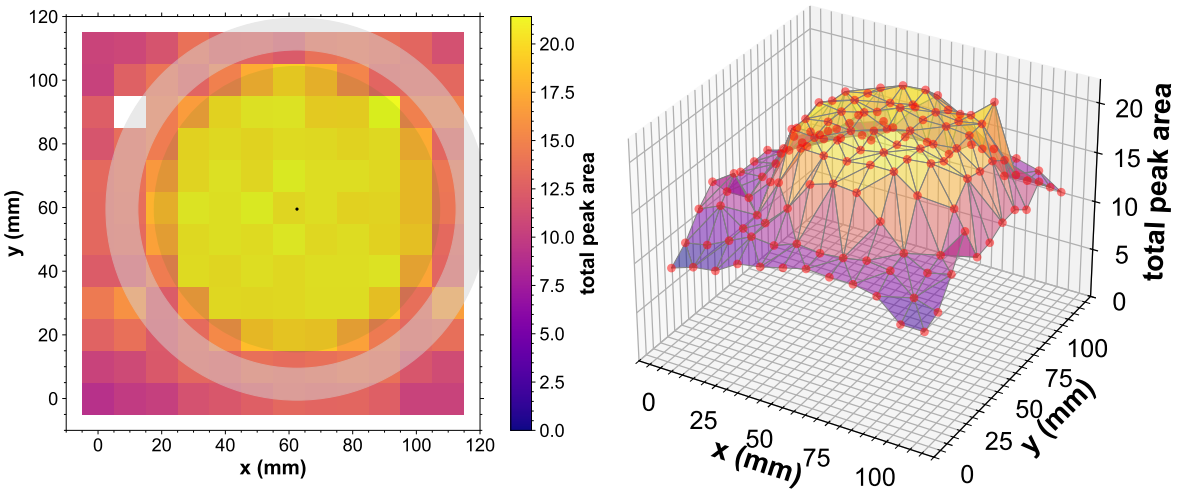

Figure 4. The acquired data for sample TP2021-008-06 with runs of 320 s. The right panel shows the same information as the left panel.

After having fitted all gamma-ray spectra, we could for each sample plot the peak area normalized to the incident neutron flux measured with the fission chamber as a function of the sample position (x, y). This is shown in the left panel of figure 4. This spectrum is not corrected for background.

The size of the cells corresponds to the dimensions of the adjustable collimator slits. The actual beam dimensions incident on the sample were slightly larger. The slit was set at 5×5 mm^2 at the start of the measurement and changed to 10×10 mm^2 for the remaining measurements in order to optimize the counting statistics. In case of an occasional bad fit, the cell of the position stays empty.

The position of the measured sample is shown on top of this figure. In particular the support ring with internal diameter R_{int}, external diameter R_{ext}, and the circular spot of the ^{10}B deposit with diameter R_B are visible. The middle of the sample is shown as a black dot. The position of the middle with respect to the scanning system was determined by a small piece of $^{10}B_4C$ positioned in the middle of an empty sample holder and determined with a beam imager.

The 3D plot in the right panel of figure 4 shows the same information with a triangular surface plot in order to appreciate the variability of the peak area. In the following we will only show the left panel figure for the measured samples.

Then we calculated the radial distance of each cell center to the center of the sample. The vertical line shows the radius of the ^{10}B deposit. Now not only the total peak area is shown, but also the measured background of one of the several empty backing measurements. For the

final results, we took a background that is the weighted mean of all background measurements. We did not multiply the uncertainty with the Birge factor (the square root of the reduced chi-square) for these means, which was ranging between 0.9 and 1.8 and not considered statistically significant.

The points with a radius R smaller than $0.75R_B$, to ensure to include only points where the beam fully hits the boron deposit, were used to calculate the weighted mean and its uncertainty. Since we could not observe a clear indication for an inhomogeneity among the points, this mean was used as a measure of the average areal density. The figures for each sample are shown in figures 5, 6, 7, 8, 11, 9 and 10.

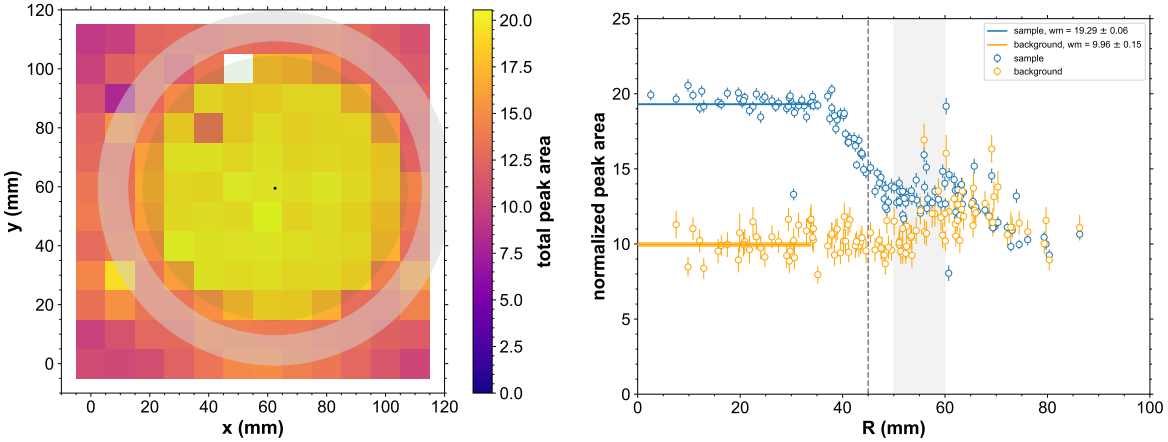

Figure 5. The acquired data for sample TP2021-008-05 with runs of 315 s.

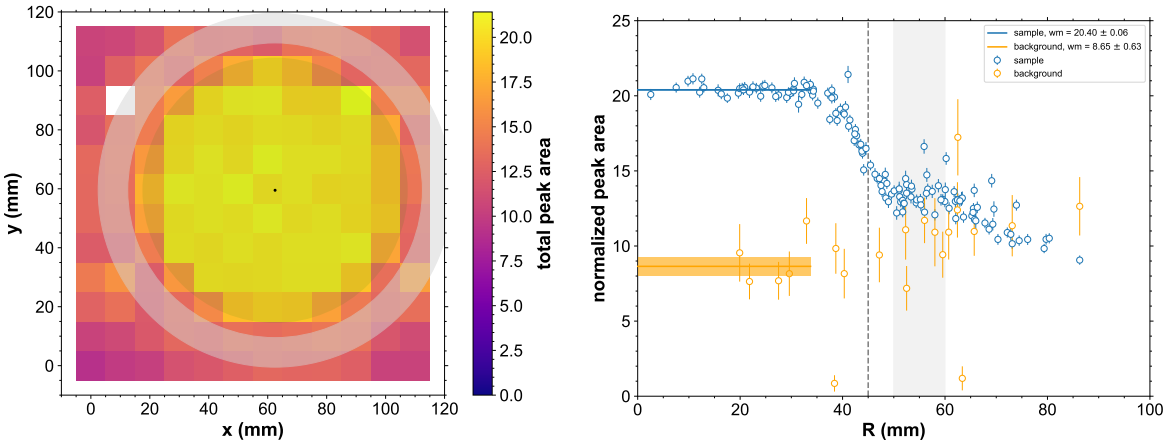

Figure 6. The acquired data for sample TP2021-008-06 with runs of 320 s.

From the weighted mean of the the normalized peak area points inside $0.75R_{\text{int}}$ and the common background, found to be coherent throughout the experiment, we calculated the net averaged normalized areas of the 478 keV peak A_{net} for each sample. From those numbers we then took the ratio $Q \pm \delta Q$ between the average net area of each sample to that of sample **TP2012-001-01**, taken as the reference sample. The ratio Q was then used to scale the reference areal density to an adopted areal density n. The numbers are shown in table 2.

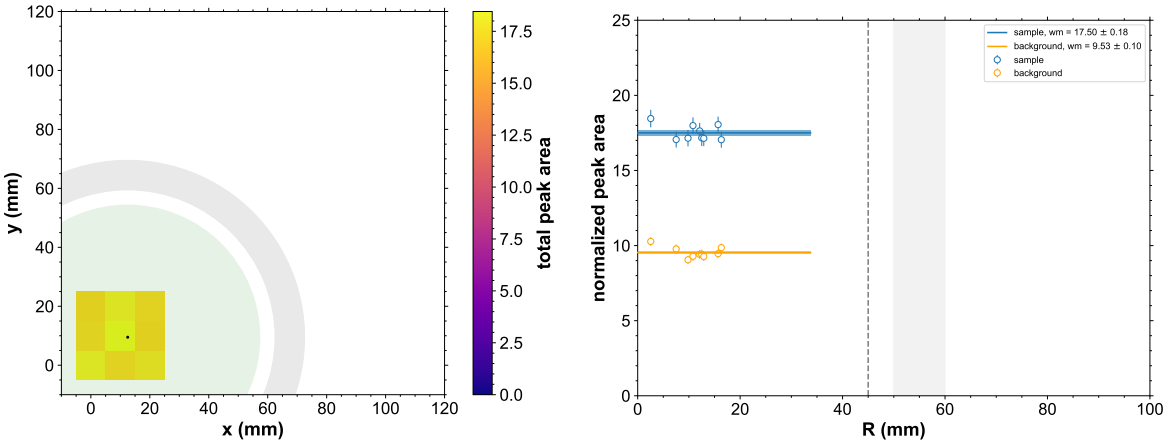

Figure 7. The acquired data for sample TP2021-008-07 with runs of 120 s.

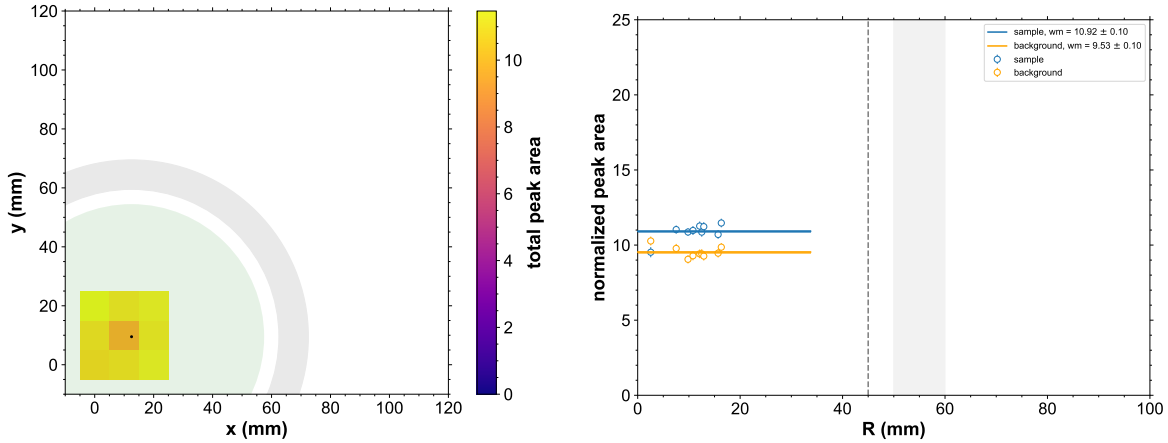

Figure 8. The acquired data for sample TP2021-008-08 with runs of 360 s.

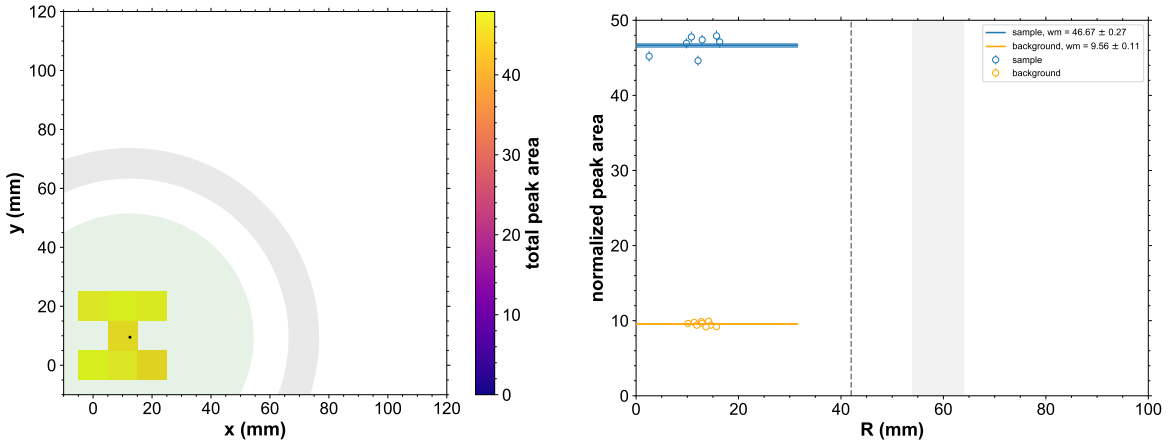

Figure 9. The acquired data for sample NS00041 with runs of 120 s.

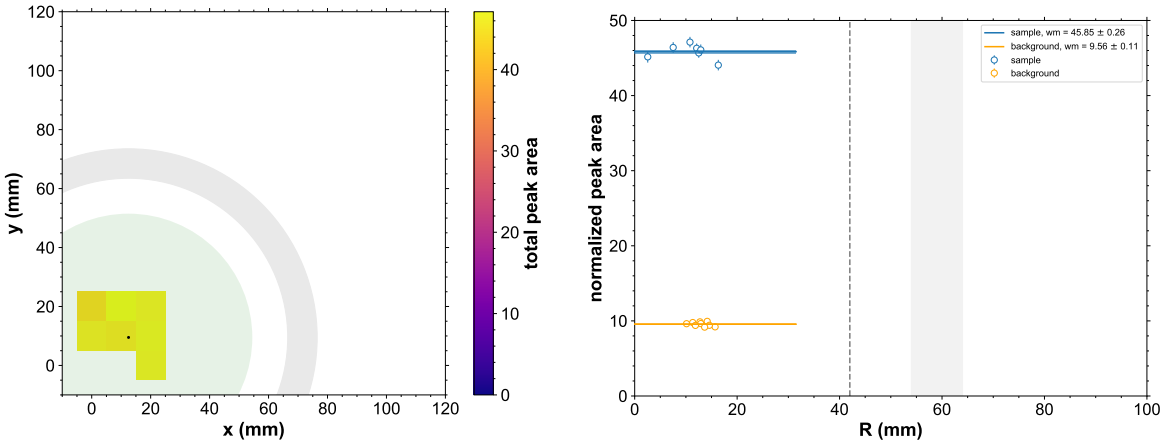

Figure 10. The acquired data for sample FP15-030 with runs of 120 s.

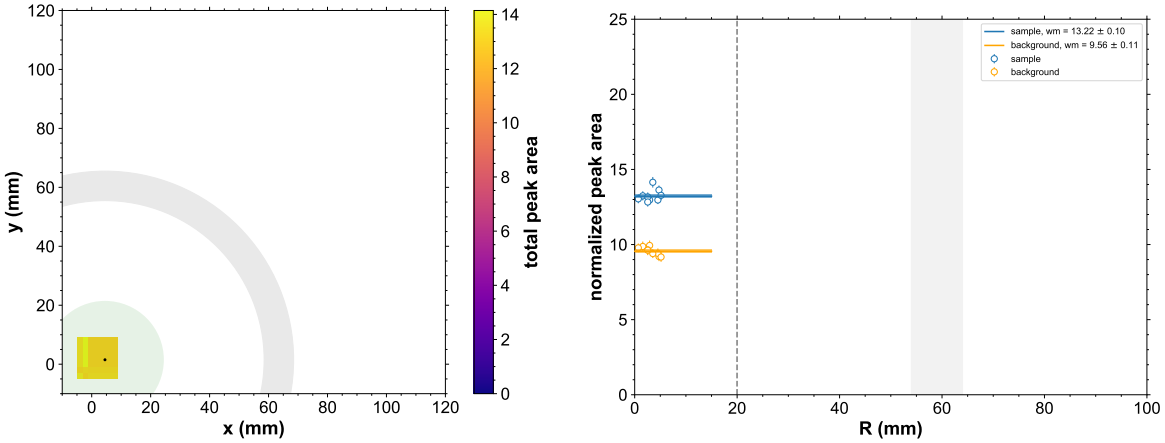

Figure 11. The acquired data for sample TP2012-001-01 with runs of 360 s.

Table 2. Values of the deduced areal density $n \pm \delta n$ for the ^{10}B samples. From the measured averaged peak area A_{tot}, normalized to the incident neutron flux, the averaged background with a value of 9.60±0.06 is subtracted to give the background subtracted peak area A_{net}. The ratio $Q \pm \delta Q$ relative to the reference sample **TP2012-001-01** is calculated, from which the adopted average areal density n is calculated for the other ^{10}B samples. Note that the final uncertainties for most samples are dominated by the background contribution to the reference sample. The δ symbol indicates one sigma uncertainties.

sample	A_{tot}	δA_{tot}	A_{net}	δA_{net}	Q	δQ	n (μg/cm^2)	δn (μg/cm^2)	δn (%)
TP2021-008-05	19.29	0.06	9.69	0.09	2.68	0.08	23.5	0.8	3.4
TP2021-008-06	20.40	0.06	10.80	0.08	2.98	0.09	26.2	0.9	3.4
TP2021-008-07	17.50	0.18	7.90	0.19	2.18	0.08	19.1	0.8	4.0
TP2021-008-08	10.92	0.10	1.32	0.11	0.36	0.03	3.2	0.3	8.5
NS00041	46.67	0.27	37.07	0.28	10.24	0.33	89.8	3.2	3.6
FP15-030	45.85	0.26	36.25	0.27	10.02	0.33	87.8	3.2	3.6
TP2012-001-01	13.22	0.10	3.62	0.12	**1**		**8.766**	**0.138**	**1.6**

4 Neutron transmission measurements

At the end of the experiment, the setup in figure 1 was slightly transformed with the goal of performing a transmission measurement. For this purpose the ^{3}He counter, which before was mounted upstream in the beam but not connected to the acquisition system, was moved to a position just behind the ^{10}B sample and connected to the acquisition system. The upstream fission chamber was kept in place and data continued to be acquired. In this configuration the $LaBr_3$ detector was kept in place.

In a transmission experiment the ratio of the incident and outgoing zero-angle neutron flux is the transmission T which is related to the total cross section by

$$T = \exp(-n\sigma_{\text{tot}}) \tag{1}$$

This ratio is experimentally measured by a same flux detector with a sample inside and outside the neutron beam.

Sample **NS00041** together with its empty backing was used for a sample-in sample-out measurement while detecting the counts in the ^{3}He detector. The counts from the ^{3}He detector were scaled to the incident neutron flux measured with the upstream fission chamber. The fission chamber and the ^{3}He detector had count rates of about 15000 and 10000 counts per second respectively. No dead time corrections could be made in this configuration.

Since the total cross section σ_{tot} of ^{10}B is 5351 b at 13.1 meV and the neutron scattering cross section only 2.3 b, the contribution from sample scattered neutrons in the detector is rather small. In the left panel of figure 12 we show the transmission as a function of the position of the sample, together with the averaged value of the transmission, both well within the radius of the boron deposit, and far outside the support ring. In the right panel of the figure 12 the same information is plotted, but now with the ^{3}He counts normalized by time instead of by the fission chamber counts.

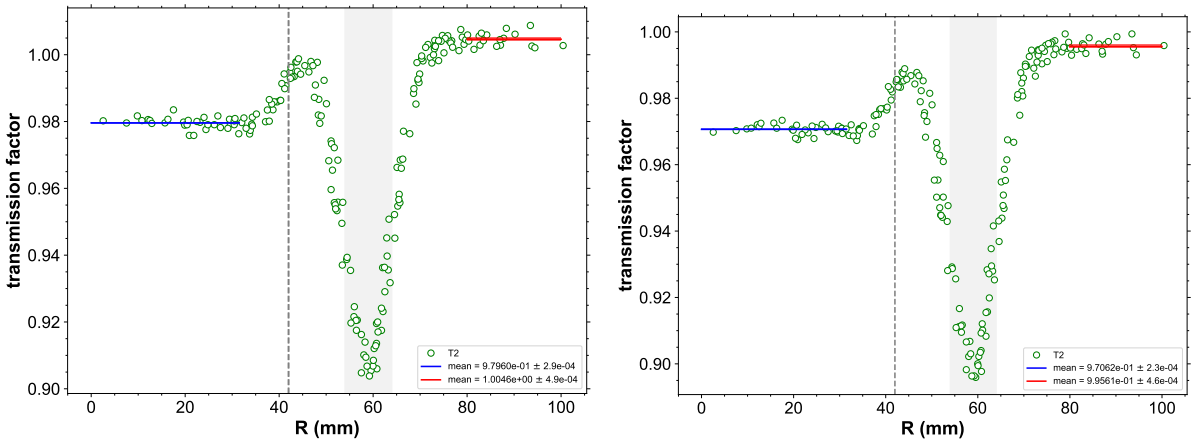

Figure 12. The acquired transmission data for sample **NS00041** with runs of 210 s. In the left panel the normalization of the ^{3}He counts is performed using the fission chamber counter, in the right panel the normalization is done by measurement time. The position of the support ring is shown as the gray band, and the radius of the boron deposit as the dashed line. The weighted means are taken over the points they cover.

Using the weighted mean of the transmission normalized by flux, which is the preferred way to normalize, we obtain approximately 64 μg/cm^2 of ^{10}B, while if we use the transmission normalized by time, which is not recommended, we obtain 93 μg/cm^2 of ^{10}B. While this number is merely by chance close to the value in table 2, a number of observations must be made.

The neutron wave length has a spread around 2.5 Å in the order of 10%. The kinetic energy of the neutrons has an according distribution, not necessarily symmetric, and the measured transmission is an average transmission $\langle T \rangle$, and it should be realized that the relation to the average total cross section is less straightforward taking in account that $\langle \exp(-n\sigma_{\text{tot}}) \rangle \neq \exp(-n\langle \sigma_{\text{tot}} \rangle)$. Moreover, no background corrections for the sample in and sample out counts have been applied, nor have any dead time corrections. Even if the total cross section for aluminium at 13.1 meV is only 1.8 b, the thickness of the backing, documented as 30 μm, might be different than the one of the ^{10}B deposit. In this case, this effect can only be rather small since a thickness of 30 μm of Al corresponds to a transmission of 0.9997. The transmission of the thin ^{10}B layer can also be sensitive to local irregularities of the areal density on a microscopic scale, to which a capture experiment is not sensitive. Finally, for these reasons we have concluded that the present measurement cannot be considered conclusive.

Conclusion

The present setup has allowed to measure the relative ^{10}B content of several samples, using a reference sample. The results are shown in table 2. The scanning device has proven to reliably work with the large diameter samples typically used in several neutron facilities. The method of gamma-ray spectroscopy is very sensitive, also for thin deposits. Since the used experimental area contained a large quantity of ^{10}B, not only in the neutron beam collimators, but also as a cladding on a nearby wall, this sensitivity resulted in a large background in the present experiment, were the quantity to be determined was the amount of ^{10}B. Concerning the homogeneity of the samples, the reduced chi-squared value of the weighted mean of the net peak area at different positions was not deviating enough from 1 to be statistically significant. Therefore we could not conclude that any of the samples were in homogeneous in the areal density. The here employed method can be used to characterize future ^{10}B samples, preferably with improved background conditions and shielding.

The test of the transmission experiment to access the total cross section was also valuable, even if not conclusive. A transmission experiment is in principle an absolute measurement, but requires a homogeneous sample, careful background subtractions and characterization of the backings, and accurate flux measurements including dead time corrections. An improved control of the flux measurements will benefit possible future measurements.

Acknowledgements

The authors would like to thank the ILL staff for the smooth operation of the reactor. JRC and CEA acknowledge support from the French *Agence Nationale de la Recherche* under contract number ANR-20-CE31-0008-01.